Optimization of RF sputtering process parameters on electrical resistivity, deposition rate and sensitivity of Al-doped ZnO thin films grown on Si substrate using grey-Taguchi technique

M VANMATHI[1],* , **M MOHAMED ISMAIL[1]** and **M SENTHIL KUMAR[2]**

[1]School of Electrical and Communication Sciences, B S Abdur Rahman Crescent Institute of Science and Technology, Chennai 600048, India
[2]School of Mechanical and Building Sciences, Vellore Institute of Technology, Chennai 600127, India
*Author for correspondence (vanmsen@yahoo.co.in)

Abstract. Increasing environmental pollution globally demands gas sensors for monitoring urban air quality, fire and exhaust from automobiles. The need for high performance gas sensors requires a good control over sensing material structure. This paper studies the suitability of Al-doped ZnO thin films for development of CO gas sensors. Deposition of Al-doped ZnO thin films on Si substrates by the radio frequency sputtering technique was carried out to study the influence of process parameters. The process parameters selected for the analysis were power, deposition time, substrate temperature and working pressure. An orthogonal array L16 (4^4), signal-to-noise ratio and analysis of variance (ANOVA) were performed to optimize the electrical resistivity, deposition rate and sensitivity of the thin films using the Taguchi method. Grey relational grade (GRG) was performed to obtain multiple-performance characteristics of the thin films by optimizing the process parameters. GRG analyses identified the process parameters: power 150 W, deposition time 35 min, substrate temperature 25°C and working pressure 1.5 Pa showed optimal multiple-performance characteristics. ANOVA analyses indicate that power and substrate temperature show significant effect compared with other parameters. Thin films at the annealing temperature (450°C) showed a decrease in electrical resistivity and an increase in sensitivity. At the sensor operating temperature of 150°C, Al-doped thin films exhibited the lowest resistivity 3.76×10^{-3} Ω-cm and the highest sensitivity of 59%. The optimal multiple-performance characteristic of thin film sample identified is found suitable for CO gas-sensing applications.

Keywords. Al-doped ZnO; thin films; resistivity; deposition rate; sensitivity.

1. Introduction

Global concern for environmental pollution caused by the industries and automobiles demanded the need for development of gas sensors to monitor toxic and combustible gases. A sensor works on the change in conductivity due to the exposure of target gases at moderate temperatures [1]. It converts the chemical quantities into electrical energy [2]. The various metal oxides used in thin films are ZnO, In_2O_3, CdO, TiO_2 and SnO_2. Among the various oxides, SnO_2 and ZnO thin films show good potential as gas sensors in detecting poisonous gases [3–5]. SnO_2 rutile tetragonal structure possessing 3.6 eV band gap energy leads to better electrical conductivity. ZnO possessing a band gap of 3.4 eV shows low resistivity, and is less toxic, comparatively low cost and chemically stable [6]. Hence, ZnO stands as a promising material for gas sensors. It is sensitive to gases such as hydrocarbons [7], H_2 [8], oxygen [9,10], H_2O [11], CO [12] and NO_2 [13].

 ZnO thin films show high resistivity, low sensor response, selectivity and the optimum operating temperature exceeds

200°C [14–16]. To study the performance of semiconductor gas sensors, these characteristics need to be analysed. ZnO doped with other elements shows improvement in selectivity and sensitivity [17]. Dopants such as Al, In, Cu, Sn, etc., added with low concentration, reduced the resistivity and improved the selectivity of different gases [18]. Al (1 at%)-doped ZnO thin films annealed at 500°C revealed a noteworthy decrease in the electrical resistance [19]. Al (1 at%)-doped ZnO thin films show significant improvement in the CO gas sensitivity at temperatures between 250 and 300°C, chemical stability and also decreased the resistivity [20]. Sensitivity reported at temperatures between 400 and 500°C is high due to the high activation energy present [21–23]. The major disadvantage is at high temperatures; gases ignite [20] leading to oxide grain growth, which affects the stability. Annealing at low temperatures affects the crystalline quality of thin films that increase the electrical resistance [24].

 ZnO thin films can be fabricated by using different techniques such as sol–gel process [25], spray pyrolysis [26], chemical vapour deposition [27], pulse laser deposition [28]

and sputtering [29]. Each and every process has its own advantages and disadvantages. Radio frequency (RF) sputtering [30] process provides a unique characteristic of producing good quality thin films at low working temperature, better surface roughness and low cost. The quality of the film deposited can be assessed by examining the process parameters in detail. Taguchi technique offers the unique advantage of studying the process parameters with limited number of experiments to optimize using appropriate design of the orthogonal array [31]. Recently, the industries have started using the Taguchi method [32] to improve the product quality. Thus, researchers have attempted to use the Taguchi method to propose the experimental design to optimize the process parameters.

For the deposition of thin films by RF sputtering, experiments designed were studied by considering the following factors: power, working pressure, oxygen ratio, annealing temperature and deposition time [33–35]. Significant outcome on the deposition rate and resistivity was observed in power, working pressure, temperature of substrate and deposition time [34,35]. Though enough research has been carried out on Al-doped ZnO thin films, very few studies have reported the single performance characteristics. The determination of multiple-performance characteristics of the thin film to study the effect of electrical resistance and sensing behaviour is worth the investigation.

Thus, this work attempts the fabrication of Al-doped ZnO thin films on a Si substrate. Taguchi technique is applied to optimize the process parameters to study electrical resistance, deposition rate and sensitivity. Factors considered were power, deposition time, substrate temperature and working pressure. The multiple-performance characteristics of the thin film process parameters were optimized by using Taguchi-grey technique.

2. Experimental

P-type (100) polished silicon wafer (diameter 50.8 mm and thickness 275 μm) was used for the deposition of Al-doped ZnO thin films by using an RF magnetron sputtering system. The commercially available pure aluminium powders (Merck, purity 99.995%) with ZnO (Merck, >99%) were mixed in a ratio of ZnO:Al 99:1 at%. The powders were ball-milled for 3 h to obtain uniform mixing and pressed (figure 1) to obtain green compacts with 50 mm diameter and 6.35 mm thickness (figure 2). Green compacts were finally sintered at 1200°C. Power, deposition time, substrate temperature and working pressure were the control factors selected as the process parameters and each had four levels to be varied. Table 1 shows the conditions for deposition and process parameter levels. A standard L16 orthogonal array with four rows and four columns was used in the Taguchi experimental design [36]. Electrical resistivity, deposition rate and sensitivity were the

Figure 1. Die used for target preparation.


Figure 2. Sputtering target.

performance characteristics to estimate Al-doped ZnO thin films.

Acetone was used to clean Si wafers thoroughly and rinsed in ethanol for 10 min prior to the deposition. To remove the contamination, the target was pre-sputtered at a 25 W power for 10 min before the deposition. High purity argon was used as a sputtering gas. Film thickness measurements were performed by using a Horiba Jobin Yvon Uvisel^{TM} spectroscopic ellipsometer with a rotating polarizer. The responding CO sensing surface is of 4.5×4.5 mm area positioned between the two pads as shown in figure 3. Sensitivity was measured at 400°C using a static gas sensing system. The metred quantity of CO gas was injected into the system using a syringe. A 5 V fixed voltage was applied to the film to record the response using a picoammeter until a steady state was reached. After CO gas exposure, air was allowed to pass into the test setup. Sensitivity (S) is defined as:

$$S = (R_a - R_g)/R_a, \tag{1}$$

Table 1. Al-doped ZnO process parameters and control factors' setting.

Substrate	Silicon wafers (diameter 50.8 mm and thickness 275 μm)			
Target	Al-doped ZnO (ZnO:Al, 99:1 wt%, 99.99% pure)			
Gas	Argon (purity 99.995%)			
Base pressure	6×10^{-2} Pa			
Substrate rotation	10 rpm			
Target distance	40 cm			

Symbol	Control factor	Unit	Level 1	Level 2	Level 3	Level 4
A	Power	W	150	200	250	300
B	Deposition time	min	35	40	45	50
C	Substrate temperature	°C	25	50	100	150
D	Working pressure	Pa	1.5	3	4	5
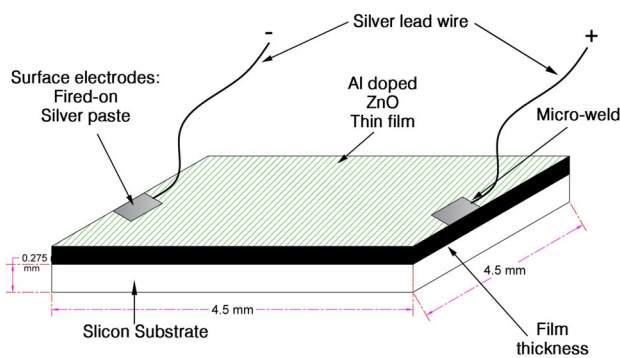
Figure 3. Schematic of CO gas sensing.

where R_g is the resistance of CO test gas and R_a the film resistance of dry air. The positive sensitivity values (S) indicate the decrease in film resistance on exposure to gas and vice versa. Thin film performance characteristics were analysed to determine the complicated interactions by grey relational analysis. The grey relational grade (GRG) is defined by the weighed summation of grey relational coefficient.

The grey relation analysis assesses the overall quality characteristics by the correlation level between the reference and the comparable sequence [37]. For computing the grey relational analysis, the optimized multi-response gets converted into a single response optimization problem. The optimized process parameters indicate that product quality is better with the highest GRG. The average grade value for each process parameter level found is shown as mean response table. The higher value of average grade value is chosen as optimal parametric combination for multi-responses. To reduce the variation of data and avoid different units, the data need to be normalized. From the original value, a suitable value is obtained between 0 and 1 to make an array [37]. This is generally a method to convert the original data to comparable data. The larger-the-better characteristics are selected for

the normalization to scale it into an acceptable range by the following formula for the response to be minimized:

$$x_i^*(k) = \frac{\max x_i(k) - x_i(k)}{\max x_i(k) - \min x_i(k)}. \tag{2}$$

If the response is larger, smaller-the-better characteristics are selected:

$$x_i^*(k) = \frac{x_i(k) - \min x_i(k)}{\max x_i(k) - \min x_i(k)}, \tag{3}$$

where $i = 1, \ldots, m$; $k = 1, \ldots, n$, m denotes the number of experimental data and n represents the number of responses. $x_i(k)$ denotes the original sequence, $x_i^*(k)$ denotes the processed data, $\max x_i(k)$ means the largest value of $x_i(k)$, $\min x_i(k)$ indicates the smallest value of $x_i(k)$ and x is the desired value [38]. The normalized value $x_i(k)$ of the kth performance characteristic is the ith experiment.

From the normalized values, grey relational coefficient $\xi_i(k)$ is calculated using the following formula:

$$\xi_i(k) = \frac{\Delta_{\min} - \xi \Delta_{\max}}{\Delta_{0i}(k) + \xi \Delta_{\max}}. \tag{4}$$

The coefficient ξ is adjusted between 0 and 1 for computing the grey relational coefficient. Generally, $\xi = 0.5$ is selected, when the parameters considered for the analysis are weighed equally.

Δ_{0i} is the deviation sequence obtained from the reference sequence and the comparability sequence

$$\Delta_{0i} = \|x_0(k) - x_i(k)\|, \tag{5}$$

where $x_0(k)$ indicates the reference sequence and $x_i(k)$ the comparability sequence; $\Delta_{\min}$ and $\Delta_{\max}$ are the absolute difference (Δ_{0i}) minimum and maximum values of all sequences

compared. Distinguishing or identification coefficient ξ range is between 0 and 1. Usually, ξ value is taken as 0.5.

The GRG is estimated using the following equation:

$$\gamma_i = \frac{1}{n} \sum_{k=1}^{n} \xi_i(k) \tag{6}$$

where γ_i is the necessary GRG for ith experiment and n the number of response characteristics.

The GRG is used to assess the effect of each parameter on multi-response that cannot be assessed by the Taguchi method. Analysis of variance (ANOVA) identified the percentage of contribution of each process parameter. Thin film predicted design using grey relational-Taguchi thin films was studied for electrical resistivity and sensitivity under different annealing conditions from 350 to 500°C at the sensor operating temperature of 200°C. The film that showed better performance was tested for its electrical resistivity and sensitivity under different sensor operating conditions (100–200°C). Surface morphologies of coated thin films were studied by using a scanning electron microscope (SEM Hitachi-S3400N). The thin film samples were characterized by using X-ray diffraction (XRD) (SEIFERT diffractometer) with CuKα radiation, $\lambda = 1.5405$ Å. Peaks measured by XRD analysis were analysed and compared with the JCPDS data.

3. Results and discussion

3.1 *Statistical analysis*

Statistical Taguchi technique is an effective tool used to optimize the process parameters used in the RF sputtering technique; it decreases the variation in the robust design of experiments [39] to produce quality products [40]. The effects on resistivity, deposition rate and sensitivity of thin films were reported. Table 1 shows the four control factors: power (A), deposition time (B), substrate temperature (C) and working pressure (D) and their four levels considered for the analysis. Therefore, an L16 (4^4) orthogonal array is selected to conduct 16 experiments. Degrees of freedom (DOF) for four factors are equal (DOF $= 16 - 1 = 15$) to 15. Taguchi method is an arithmetic technique to optimize the process parameters and it increases the quality of the deposited thin films. The response input values for electrical resistance, deposition rate and sensitivity were measured for the 16 trial settings. Optimum levels and ranking of the process factors were identified by signal-to-noise (S/N) ratio and ANOVA. Disordered parameters in the S/N ratio reduced the quality characteristic variations. S/N ratio quality characteristics considered for process optimization are the-larger-the-better, the-smaller-the-better and the-nominal-the-best. For the electrical resistance the-smaller-the-better and for deposition rate and sensitivity the-larger-the-better option were selected.

S/N ratio and ANOVA table are obtained by the method mentioned in ref. [39]:

$$\text{For the smaller-the-better, S/N} = -10 \log \frac{1}{n} \sum_{i}^{n} y_i^2. \tag{7}$$

$$\text{For the larger-the-better, S/N} = -10 \log \frac{1}{n} \sum_{i}^{n} 1/y_i^2, \tag{8}$$

where y_i is the observed response value for ith repetition and n the number of replications.

Taguchi analysis was performed using MINITAB 18. Process parameters considered were power (A), deposition time (B), substrate temperature (C) and working pressure (D) and their four levels were arranged in the L16 orthogonal array. The measured values of electrical resistance, deposition rate and sensitivity for the L16 orthogonal array with design factors are presented in table 2. S/N ratios for factors that control the deposition rate, electrical resistance and sensitivity are shown in tables 3–5. The power showed better correlation for electrical resistance, deposition rate and sensitivity.

Performance characteristics of S/N ratio identified the optimum process parameter level. The optimal response observed for the electrical resistivity (table 3) is level 1 for power, level 3 for deposition time, level 4 for substrate temperature and level 2 for working pressure, which are also presented in the S/N ratio curves (figure 4) as A1B3C3D3. Responses for deposition rate (table 4) and sensitivity (table 5) were found to be level 1 for power, level 3 for deposition time, level 2 for substrate temperature and level 4 for working pressure and their optimum process parameters are A4B3C3D4 and A3B1C3D2 (figures 5 and 6). From the analysis, it is observed that power plays a key role in the performance of electrical resistivity, deposition rate and sensitivity of the thin films. To confirm this hypothesis, ANOVA was accomplished to identify the contributions of the process parameters used in this study.

Performance characteristics of thin films that are affected by the process parameters are determined by using MINITAB 18. Computational technique was used to evaluate and compare the contributions. This is done by performing ANOVA. ANOVA is expressed as the sum of squares of the standard deviation and is equal to the sum of squares of the standard deviation produced by each and every parameter. ANOVA table obtained is as described in the previous literature [39]. Tables 6–8 show the ANOVA variance for electrical resistance, deposition rate and sensitivity, respectively. F-ratio is calculated considering the ratio between the regression mean square and the mean squared error. An increase in the F value contributes to an increase in the significance of the parameter (table 6). The power plays a significant role in electrical resistivity of thin films with 90.32% contribution ratio. The electrical resistivity was the lowest at a 150 W power. It increases with increasing power up to 250 W and marginally decreases at 300 W (figure 4). The increase in

Table 2. L16 orthogonal array with design factors and S/N ratio for electrical resistance, deposition rate and sensitivity.

Power (W)	Deposition time (min)	Substrate temperature (°C)	Working pressure (Pa)	Electrical resistance $\times 10^{-3}$ (Ω-cm)	Deposition rate (nm min^{-1})	Sensitivity (%)	S/N ratio for electrical resistance	S/N ratio for deposition rate	S/N ratio for sensitivity
150	35	25	1.5	15.95	11.5	43	−24.05	21.21	32.66
150	40	50	3	16.8	12.5	40	−24.50	21.93	32.04
150	45	100	4	18.7	14.5	39	−25.43	23.22	31.82
150	50	150	5	12.35	12.5	36	−21.83	21.93	31.12
200	35	50	4	15.23	19.5	35	−23.65	25.80	30.88
200	40	25	5	13.15	20.5	37	−22.37	26.23	31.36
200	45	150	1.5	15.21	24	38	−23.64	27.60	31.59
200	50	100	3	15.05	23.5	40	−23.55	27.42	32.04
250	35	100	5	7.15	26.5	57	−17.08	28.46	35.11
250	40	150	4	8.28	26	52	−18.36	28.29	34.32
250	45	25	3	7.42	23	46	−17.40	27.23	33.25
250	50	50	1.5	7.5	27	42	−17.50	28.62	32.46
300	35	150	3	8.25	30	40	−18.32	29.54	32.04
300	40	100	1.5	7.43	31.5	39	−17.41	29.96	31.821
300	45	50	5	7.76	35	36	−17.79	30.88	31.126
300	50	25	4	7.1	32	35	−17.02	30.10	30.88

Table 3. Response table for S/N ratio: smaller is better (electrical resistance).

Level	Power (W)	Deposition time (min)	Substrate temperature (°C)	Pressure (Pa)
1	−23.96	−20.78	−20.22	−20.65
2	−23.31	−20.67	−20.86	−20.95
3	−17.59	−21.07	−20.87	−21.12
4	−17.64	−19.98	−20.54	−19.77
Delta	6.37	1.09	0.66	1.35
Rank	1	3	4	2

electrical resistivity observed is due to the damage caused by the negative ions that collide with Al-doped ZnO thin films [40]. High power and extrinsic dopants [41] affect electrical nature. Therefore, the electrical resistance was found to be varied from 15.95 to 7.1×10^{-3} Ω-cm. The results show that power dominates the electrical resistance, followed by working pressure, deposition rate and substrate temperature that recorded their contribution ratios as 4.18, 2.43 and 1.53%, respectively. Therefore, the power gets modified within a small level according to these factors.

In the case of deposition rate, power plays a significant role and the contribution ratio amounts to 94.89% (table 7). An increase in the power increased the deposition rate, as the sputtered atoms increased proportionally [22]. Thus, the growth takes place at the surface [42]. The contribution ratios for the deposition time, substrate temperature and working pressure correspond to 1.55, 1.35 and 0.56%, respectively. The results in table 8 confirmed that sensitivity is influenced by power, which is the major contributor with 67.12%, followed by deposition time, substrate temperature and

working pressure contribution ratios of 12.51, 11.27 and 0.92%, respectively.

To summarize, the optimum performance characteristics of electrical resistivity, deposition rate and sensitivity were found to be varied individually. The objective of this research is to identify the optimal deposition parameters to obtain thin films with multiple-performance characteristics. Hence, to optimize the process parameters, grey relational analysis was selected.

Linear regression equations obtained for the electrical resistivity, deposition rate and sensitivity parameters measured from power, deposition time, substrate temperature and working pressure are:

Regression equation for electrical resistance

$$= 11.458 + 4.492A1 + 3.202A2 - 3.871A3 - 3.823A4$$
$$+ 0.187B1 - 0.043B2 + 0.814B3 - 0.958B4$$
$$- 0.553C1 + 0.364C2 + 0.624C3 - 0.436C4$$
$$+ 0.064D1 + 0.422D2 + 0.869D3 - 1.356D4. \quad (9)$$

Main Effects Plot for SN ratios
Data Means
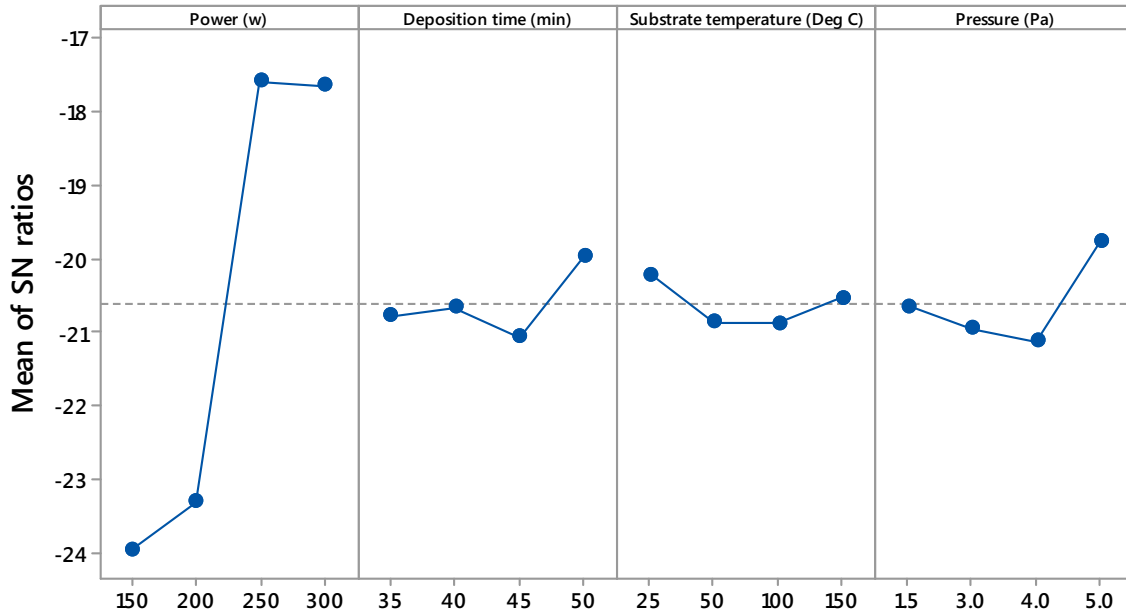
Signal-to-noise: Smaller is better

Figure 4.   S/N ratio response curve for electrical resistance.

Table 4.   Response table for S/N ratio: larger is better (deposition rate).

Level	Power (W)	Deposition time (min)	Substrate temperature (°C)	Pressure (Pa)
1	22.08	26.26	26.20	26.85
2	26.77	26.61	26.81	26.53
3	28.16	27.24	27.27	26.86
4	30.12	27.02	26.85	26.88
Delta	8.04	0.98	1.07	0.35
Rank	1	3	2	4

Table 5.   Response table for S/N ratio: larger is better (sensitivity).

Level	Power (W)	Deposition time (min)	Substrate temperature (°C)	Pressure (Pa)
1	31.91	32.68	32.04	32.14
2	31.47	32.39	31.63	32.34
3	33.79	31.95	32.70	31.98
4	31.47	31.63	32.27	32.18
Delta	2.32	1.05	1.07	0.37
Rank	1	3	2	4

Regression equation for deposition rate
$$= 23.094 - 10.344A1 - 1.219A2$$
$$+ 2.531A3 + 9.031A4$$
$$- 1.219B1 - 0.469B2 + 1.031B3 + 0.656B4$$
$$- 1.344C1 + 0.406C2 + 0.906C3 + 0.031C4$$
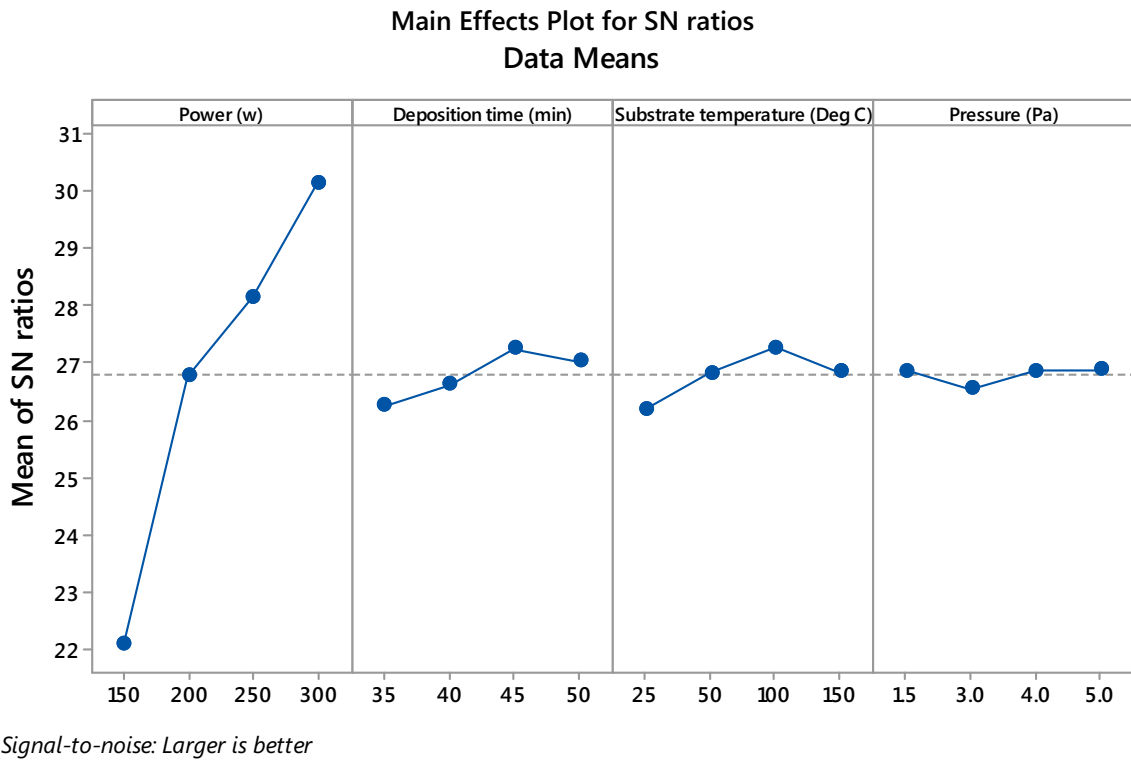$$+ 0.406D1 - 0.844D2 - 0.094D3 + 0.531D4. \quad (10)$$

Main Effects Plot for SN ratios
Data Means

Signal-to-noise: Larger is better

Figure 5. S/N ratio response curve for deposition rate.

Main Effects Plot for SN ratios
Data Means
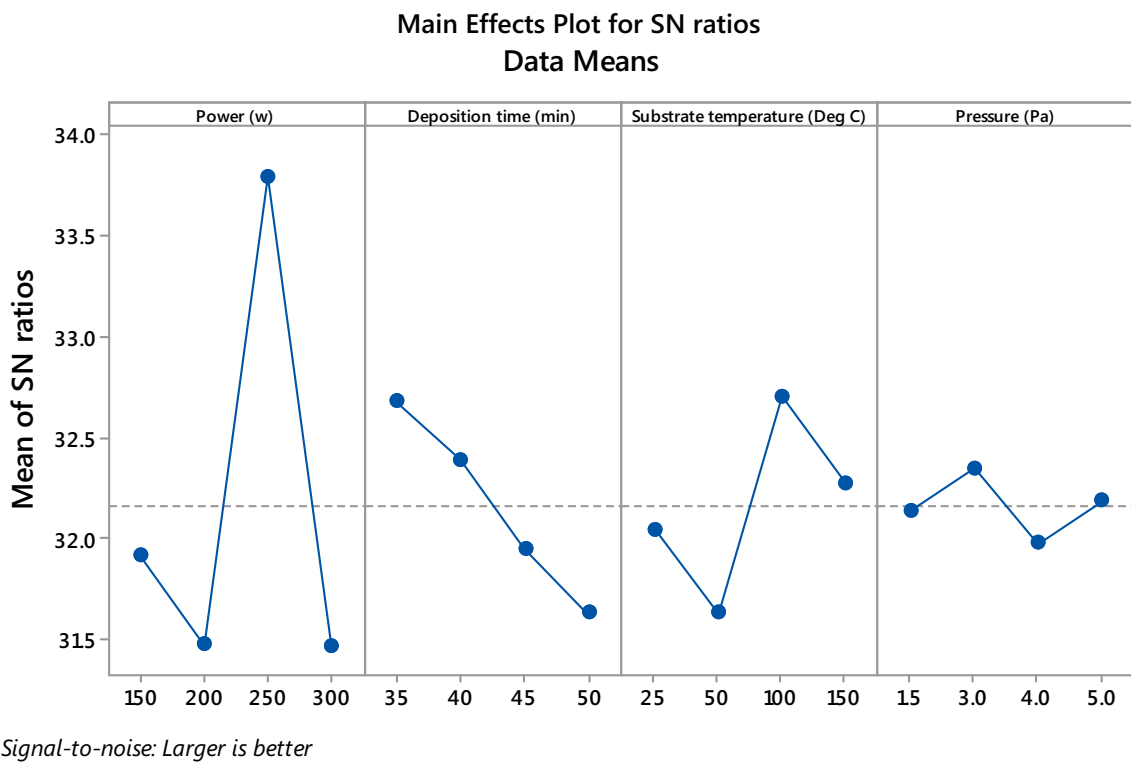

Signal-to-noise: Larger is better

Figure 6. S/N ratio response curve for sensitivity.

Table 6. ANOVA variance table for electrical resistance.

Source	DF	Seq. SS	Contribution (%)	Adj. SS	Adj. MS	*F* value	*P* value
Power (W)	3	240.108	90.32	240.10	80.03	58.77	0.004
Deposition time (min)	3	6.472	2.43	6.47	2.15	1.58	0.357
Substrate temperature (°C)	3	4.073	1.53	4.07	1.35	1.00	0.501
Working pressure (Pa)	3	11.103	4.18	11.10	3.70	2.72	0.217
Error	3	4.085	1.54	4.085	1.36		
Total	15	265.841	100.00				

Table 7. ANOVA variance table for deposition rate.

Source	DF	Seq. SS	Contribution (%)	Adj. SS	Adj. MS	*F* value	*P* value
Power (W)	3	785.79	94.89	785.79	261.93	57.48	0.004
Deposition time (min)	3	12.797	1.55	12.79	4.26	0.94	0.521
Substrate temperature (°C)	3	11.172	1.35	11.17	3.72	0.82	0.564
Working pressure (Pa)	3	4.672	0.56	4.67	1.55	0.34	0.799
Error	3	13.672	1.65	13.67	4.55		
Total	15	828.10	100.00				

Table 8. ANOVA variance table for sensitivity.

Source	DF	Seq. SS	Contribution (%)	Adj. SS	Adj. MS	*F* value	*P* value
Power (W)	3	379.18	67.12	379.18	126.39	8.21	0.059
Deposition time (min)	3	70.68	12.51	70.68	23.56	1.53	0.368
Substrate temperature (°C)	3	63.68	11.27	63.68	21.22	1.38	0.399
Working pressure (Pa)	3	5.18	0.92	5.18	1.72	0.11	0.947
Error	3	46.18	8.18	46.18	15.39		
Total	15	564.93	100.00				

Regression equation for sensitivity

$$= 40.938 - 1.44A1 - 3.44A2 + 8.31A3 - 3.44A4$$
$$+ 2.81B1 + 1.06B2 - 1.19B3 - 2.69B4$$
$$- 0.69C1 - 2.69C2 + 2.81C3 + 0.56C4$$
$$- 0.44D1 + 0.56D2 - 0.69D3 + 0.56D4 . \quad (11)$$

3.2 *Grey relational analysis*

Measured values of electrical resistance, deposition rate and sensitivity for the L16 orthogonal array (table 2) were used to calculate the GRG. Grey relational analysis shows the association between the comparable sequence and the reference sequence. The designed GRG varies between 0 and 1. When two sequences are identically coincident, it equals 1. From the ANOVA and grey relational analysis, possibility exists to obtain the optimal combinations for the thin films. To assess the multiple-performance characteristics of thin

films, electrical resistivity, deposition rate and sensitivity were considered. Single GRG was calculated considering equations (2–6). Grey relation coefficient and GRG obtained from the experiments using the L16 orthogonal array are shown in table 9. The results obtained were ranked. The highest value in the GRG L16 experiment is assumed close to the normalized value. It represents the key performance characteristics. The Taguchi method showed the GRG value of 0.795 as the highest among the 16 trials that corresponds to A1B1C1D1. It represents the optimal multiple-performance characteristics in the L16 array.

It is evident from figure 7, grey theory prediction design from the S/N ratio for the GRG combination set A1B1C1D1 showed multiple-performance characteristics. Corresponding responses (table 10) for GRG identified levels 1 for power, 3 for deposition time, 2 for substrate temperature and 4 for working pressure. The observation shows that the predicted design is similar to the obtained orthogonal array parameter (table 9). Contributions of each process

Table 9. Grey relation grade with ranking.

Run	Evaluation of Δ_{0i}			Grey relation coefficient				
Ideal sequence	Electrical resistance $\times 10^{-3}$ (Ω-cm)	Deposition rate (nm min^{-1})	Sensitivity (%)	Electrical resistance $\times 10^{-3}$ (Ω-cm)	Deposition rate (nm min^{-1})	Sensitivity (%)	Grey relation grade	Rank
1	0.802	0.000	0.000	0.384	1.000	1.000	0.795	1
2	0.863	0.029	0.143	0.367	0.922	0.778	0.689	2
3	1.000	0.086	0.257	0.333	0.797	0.660	0.597	10
4	0.543	0.029	0.343	0.479	0.922	0.593	0.665	3
5	0.750	0.229	0.371	0.400	0.595	0.574	0.523	13
6	0.601	0.257	0.429	0.454	0.566	0.538	0.520	14
7	0.749	0.357	0.457	0.400	0.485	0.522	0.469	15
8	0.737	0.343	0.514	0.404	0.495	0.493	0.464	16
9	0.025	0.429	1.000	0.952	0.439	0.333	0.575	12
10	0.035	0.414	0.857	0.935	0.448	0.368	0.584	11
11	0.045	0.329	0.686	0.918	0.505	0.422	0.615	6
12	0.050	0.443	0.571	0.908	0.431	0.467	0.602	9
13	0.032	0.529	0.514	0.939	0.388	0.493	0.607	8
14	0.000	0.571	0.486	1.000	0.370	0.507	0.626	5
15	0.032	0.671	0.400	0.939	0.333	0.556	0.609	7
16	0.022	0.586	0.371	0.959	0.364	0.574	0.632	4

parameter assessed from the results of GRG predicted, are presented in ANOVA (table 11). Power (A) being the major contributor, obtained the optimal multiple-performance characteristics in the thin film with 75.54%, followed by substrate temperature (C) with 12.68% which is slightly higher than deposition time (B) with 5.85% and pressure (D) with 3.45%. The optimal deposition parameters (A1B1C1D1) to obtain thin films are 150 W power, 35 min deposition time, 20°C substrate temperature and 1.5 Pa working pressure. The electrical resistivity measured at the lowest deposition rate 11.5 nm min^{-1} was 15.95×10^{-3} Ω-cm from the grey theory prediction design. Grey relational analyses simplified the optimization of complicated thin films with multiple-performance characteristics. Therefore, the integration of grey relational analysis and the Taguchi technique optimized the process parameters contributing to the improved process efficiency.

Linear regression equations obtained for GRG measured from power, deposition rate, substrate temperature and working pressure are:

$$
\begin{aligned}
\text{Regression equation GRG} \\
= 0.59825 + 0.0883\text{A1} - 0.1042\text{A2} \\
- 0.0043\text{A3} + 0.0202\text{A4} + 0.0268\text{B1} \\
+ 0.0065\text{B2} - 0.0257\text{B3} - 0.0075\text{B4} \\
+ 0.0423\text{C1} + 0.0075\text{C2} - 0.0327\text{C3} - 0.0170\text{C4} \\
+ 0.0248\text{D1} - 0.0045\text{D2} - 0.0142\text{D3} - 0.0060\text{D4}.
\end{aligned}
$$
$$(12)$$

3.3 *Response and resistivity of sensors for CO gas measurement*

The response and resistivity of thin films were studied for CO gas injected at 100 ppm for the sample A1B1C1D1 under different annealing conditions. Figure 8 shows the Al-doped ZnO thin films subjected to study of the electrical resistivity and sensor response at different annealing temperatures from 350 to 500°C. It is observed that maximum sensitivity to CO gas was obtained in the thin film annealed at 450°C. The results showed a decrease in electrical resistivity and an increase in sensitivity up to the annealing temperature of 450°C. Above this temperature, it was found that the resistivity increased and the sensitivity decreased marginally.

To obtain the optimum conditions, the sample A1B1C1D1 annealed at 450°C temperature was subjected to experiments for the study of electrical resistivity and the response of thin film between the sensor operating temperatures of 100 and 200°C. The electrical resistivity and sensitivity measured for different sensor operating temperatures are shown in figure 9. Electrical resistivity showed a decrease from 4.97×10^{-3} to 4.75×10^{-3} Ω-cm. The Al-doped ZnO thin film at 150°C showed the lowest resistivity of 3.76×10^{-3} Ω-cm; the reason being the substitution of Al in Zn atoms increases the concentration of free electrons which reduces the resistance of the oxide. It is well-known that the radius of Al^{3+} is smaller than that of the Zn^{2+} ions; hence the substitution of atoms becomes easy. It is concluded that electrical nature of thin films was affected by the extrinsic dopants [43] and the crystal structure of films with the growth rate [44]. The results
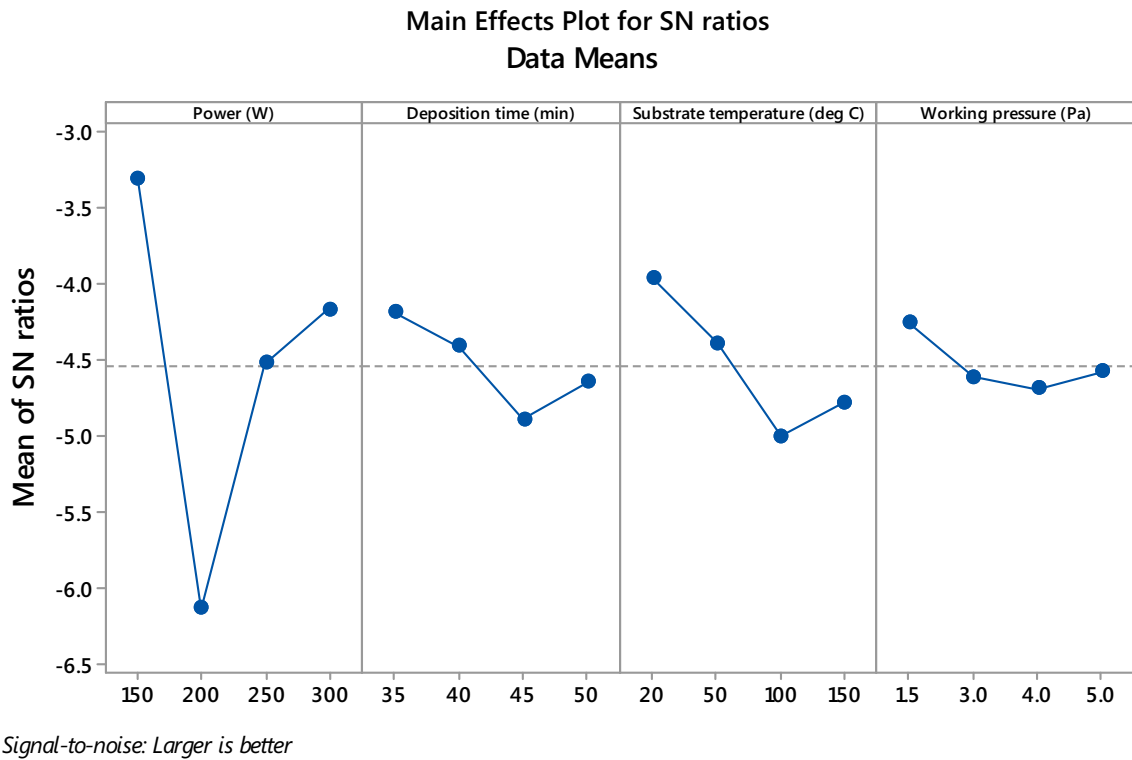
Main Effects Plot for SN ratios
Data Means

Signal-to-noise: Larger is better

Figure 7. S/N ratio response curve for grey relation grade.

Table 10. Response table for S/N ratio: larger is better (grey relation grade).

Level	Power (W)	Deposition time (min)	Substrate temperature (°C)	Working pressure (Pa)
1	−3.313	−4.191	−3.970	−4.261
2	−6.139	−4.414	−4.395	−4.616
3	−4.527	−4.897	−5.006	−4.692
4	−4.175	−4.652	−4.782	−4.584
Delta	2.826	0.705	1.036	0.431
Rank	1	3	2	4

Table 11. ANOVA variance table for grey relation grade.

Source	DF	Seq. SS	Contribution (%)	Adj. SS	Adj. MS	*F* value	*P* value
Power (W)	3	0.076337	75.54	0.076337	0.025446	30.38	0.010
Deposition time (min)	3	0.005909	5.85	0.005909	0.001970	2.35	0.250
Substrate temperature (°C)	3	0.012812	12.68	0.012812	0.004271	5.10	0.107
Working pressure (Pa)	3	0.003488	3.45	0.003488	0.001163	1.39	0.397
Error	3	0.002513	2.49	0.002513	0.000838		
Total	15	0.101057	100.00				

of the SEM analysis confirmed the growth of grains with the increase in annealing temperatures. Therefore, a small amount of Al doped into ZnO provides excess electrons that decreased the electrical resistivity by 26.3%.

The sensitivity of the thin films increased from 55 to 57% between the operating temperatures of 100 and 200°C (figure 9). Maximum sensitivity was observed at 150°C; it showed an effective catalytic reaction and the decrease in the resistivity on exposure to CO gas. This led to an increase in the sensitivity by 59%, attributed to limited reaction sites existing on the film surface. The highest sensitivity achieved was 59% and it showed an overall 33% improvement in the annealed samples. It is also observed that doping Al into the ZnO increased the stacking fault density. This is a type
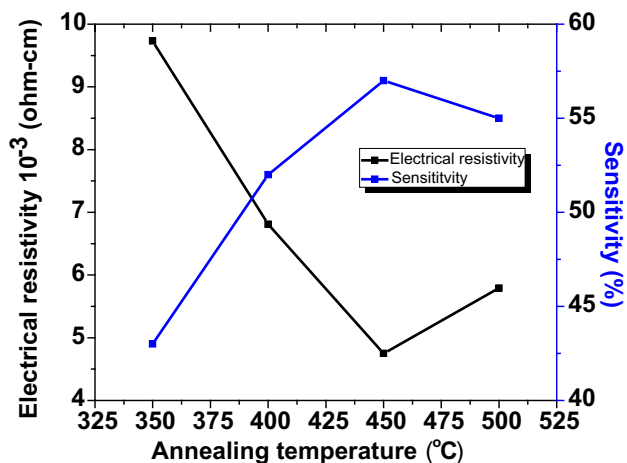
Figure 8. Resistivity and sensitivity plotted as a function of annealing temperature for Al-doped ZnO thin films.
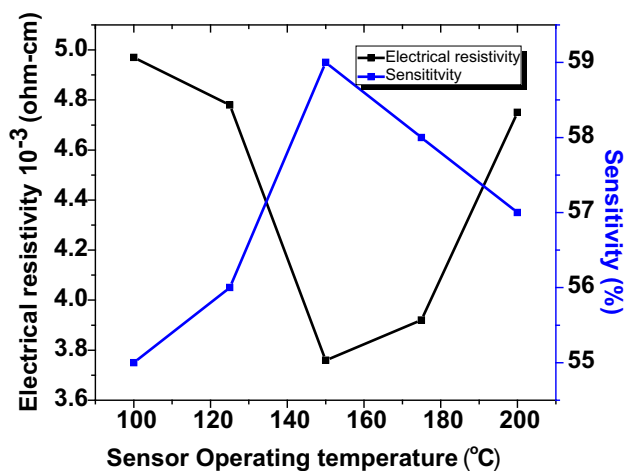

Figure 9. Resistivity and sensitivity plotted as a function of sensor operating temperature for Al-doped ZnO thin films at the annealing temperature of 450°C.

of defect in the form of oxygen vacancy that modifies the electronic properties of thin films. It alters the surface interaction of Al-doped ZnO thin films. The presence of stacking fault defects leads to performance improvement, and plays a key role in the performance of a thin film for gas sensing application. The electrical resistivity and sensitivity measured at 150°C showed optimum results. It indicates the highest thermal energy required to activate the material for progress in reaction. Above this operating temperature, resistivity and sensitivity showed a reverse trend as the oxygen adsorbents are desorbed from the surface of the sensor [45].

The CO gas sensing characteristics of ZnO-based sensors presented in table 12 show that the sensitivity obtained in this work is substantial compared with Al-doped ZnO and ZnO-based thin film sensors [46,47]. Thus, the results indicate maximum sensitivity of the thin film is achieved at 100 ppm CO gas at 150°C; it is due to quick oxidation of gases.

Table 12. CO gas sensing characteristics of ZnO-based sensors.

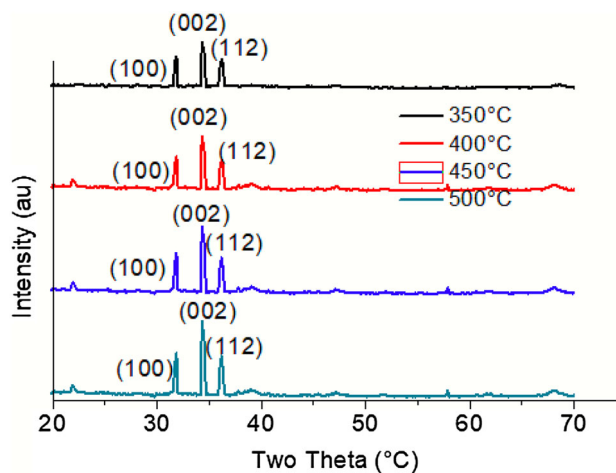| Sample	Sensitivity response (%)	CO (ppm)	Operating temperature (°C)	Ref.
Al/ZnO	57	100	150	This work
Al/ZnO	50	200	300	[20]
Cu/ZnO	48	20	300	[32]

Figure 10. XRD pattern for Al-doped ZnO (1 wt.% Al) thin film for grey theory predicted design at different annealing temperatures, 350, 400, 450 and 500°C.

Therefore, the resistivity and sensitivity results obtained show the process parameter optimized sample A1B1C1D1 is suitable for CO gas sensing application at 150°C.

3.4 Comparison of effect of thin film deposition on substrate and annealing temperature at 350°C

To study the influence of Al-doped ZnO thin films on the electrical resistance and sensing properties at the operating temperature 150°C, it is important to investigate the sensing and electrical resistance of the thin films at the substrate and the annealing temperature of 350°C. The electrical resistivity and sensitivity obtained for Al-doped ZnO thin films prepared with deposition parameters; power (150 W), deposition time (35 min), substrate temperature (350°C) and working pressure (1.5 Pa) were 4.22×10^{-3} Ω-cm and 43%. The multiple-performance characteristics of thin film sample A1B1C1D1 annealed at 350°C subjected to resistivity and sensitivity, displayed 4.76×10^{-3} Ω-cm and 44%. On comparison, it is found that the thin film annealed at 350°C showed better performance. The decrease in resistivity of the film was due to the decrease in the grain boundaries and crystal deficiencies [48]. Also, annealing produces a dense and homogeneous
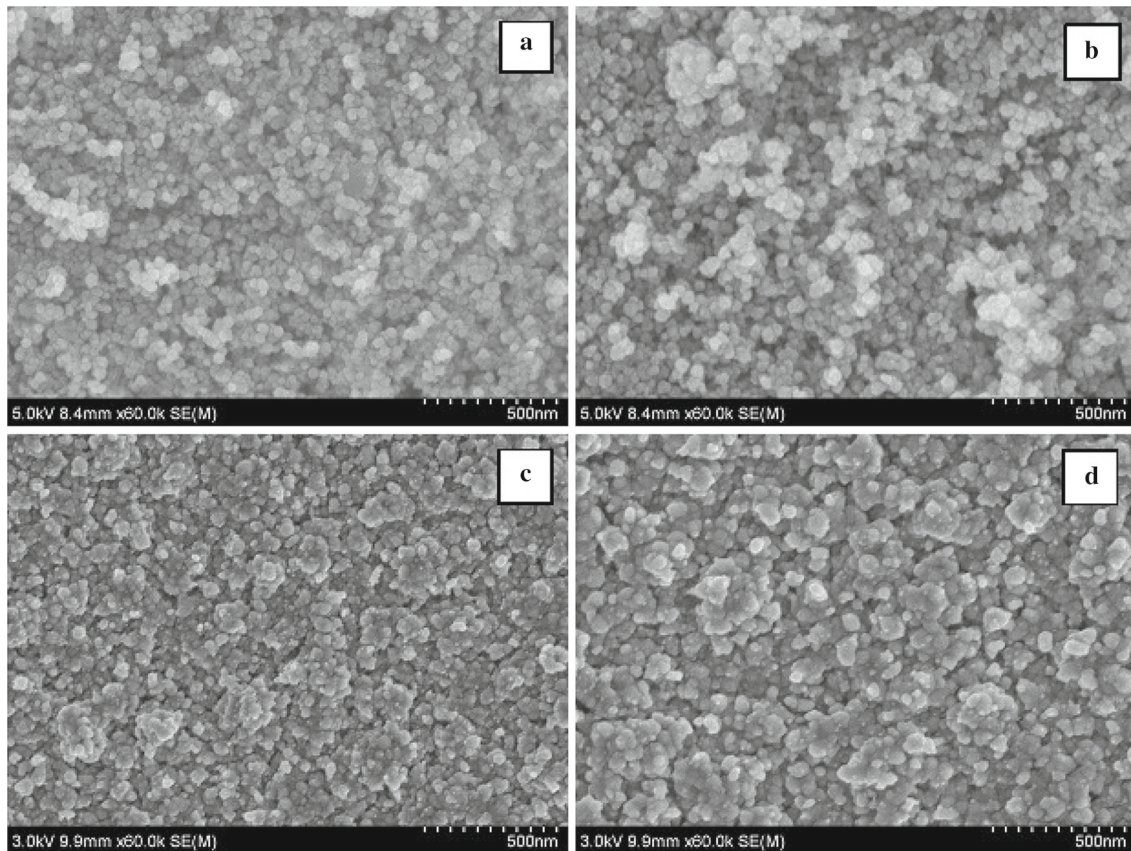
Figure 11. Microstructure of Al-doped ZnO thin films for grey theory predicted design at different annealing temperatures, (**a**) 350, (**b**) 400, (**c**) 450 and (**d**) 500°C.

thin film. Thus, the grain growth occurs which is due to the coalescence produced by heat treatment. Al-doped ZnO thin films' defects, such as Zn interstitials and oxygen vacancies at the grain boundaries [49,50] are most favourable to the coalescence process that induces larger grains [46]. In the case of thin films prepared at the substrate temperature of 350°C, deposition could have happened with controlled grain growth and random orientations.

In conclusion, electrical resistance and sensing properties of the Al-doped ZnO thin films are closely related to the post-heating temperature. Hence, it is significant that annealing improves the crystallinity, electrical resistance [51] and sensing properties of the Al-doped ZnO thin films.

3.5 *Microstructure analysis*

3.5a *Phase evolution*:   XRD patterns of Al-doped ZnO thin films on P-type silicon (1 0 0) wafer substrate for different annealing temperatures are shown in figure 10. Peak intensities observed at (1 0 0), (0 0 2) and (1 1 2) with the strong diffraction (0 0 2) indicated Wurtzite hexagonal structure which is the preferred crystal orientation on the Si

substrates [52]. It is found that the XRD pattern matched JCPDS no. 01-070-8072. The results obtained were substantial [53]. It can be noticed from the pattern that the angle of diffraction shifted marginally from 34.43 to 34.32°. This slight deviation in the position (0 0 2) to a lower angle was due to the dopant Al^{3+}. The Al atoms substituting the Zn atoms reported the presence of compressive stress parallel to the surface [54]. Thus, there was an increased interplanar spacing and this phenomenon might have led to the decreased diffraction angle [54]. It is seen that the intensity of peaks increased with an increase in annealing temperature. The peak at (0 0 2) showed the highest intensity, compared with other Al peaks. It indicates that good crystallinity can be obtained in the sample. It should be noted that the hexagonal ZnO structure with the (0 0 2) direction is most favourable for growth plane with the lowest surface energy.

3.5b *SEM analysis*:   Figure 11a–d shows the SEM images of the thin film at different annealing temperatures. The micrograph showed significant differences in surfaces between the films and coarse morphology. It could be mainly due to the agglomeration of nanoparticles. However, the thin films

represented in figure 11a and b showed more dense or thick nature. Also it can be seen in the micrograph that the absence of Al at few locations for the annealing temperatures 350 and 400°C. The observation showed that films represented rod-like structure with uniform size distribution. The average size of the ZnO and Al particles analysed from the SEM image using Image-J showed 100 and 15 nm [55]. The trend shows that the grain size tends to increase with an increase in annealing temperature (figure 11c). The results obtained were in good agreement as the lowest electrical resistivity is observed in larger grain sizes. It should be due to the reduction in electron scattering at grain boundaries and increased carrier mobility that provides a higher mean free path [56] in the thin film annealed at 450°C. At 500°C, figure 11d shows a larger grain size and increased pore volume; it restricted the carrier mobility [57], hence resistivity increases.

4. Conclusions

RF sputtering process parameter optimized Al-doped ZnO thin films have been successfully studied using the Taguchi technique based on an L16 orthogonal array by considering four factors and levels. The process parameters studied were power, deposition time, substrate temperature and working pressure. The following are the conclusions drawn:

- Taguchi analysis recognized the optimal performance characteristics of electrical resistivity, deposition time and sensitivity of thin films individually.
- Optimal combination of deposition parameter (A1B1C1D1) is 150 W power, 35 min deposition time, 20°C substrate temperature and 1.5 Pa working pressure obtained from the grey-Taguchi method identified Al-doped ZnO thin films with multiple-performance characteristics.
- ANOVA results for the GRG indicate that power significantly affects the electrical resistivity, deposition rate and sensitivity of Al-doped ZnO thin films.
- Proposed a simple regression equation for GRG measured from the power, deposition rate, substrate temperature and working pressure.
- Microstructural analysis showed a rod-like structure with uniform size distribution.
- Thin films annealed at 450°C exhibited the lowest resistivity of 3.76×10^{-3} Ω-cm and the highest sensitivity of 59%.

The Al-doped thin film sample noticeably improved CO gas sensitivity, and is found favourable for the future development of sensor devices for practical applications.

Acknowledgements

References

[1] Seiyama T, Kato A, Fjiishi K and Nagatani M 1962 *Anal. Chem.* **34** 1502

[2] Shi J, Li J, Zhu Y, Wei F and Zhang X 2002 *Anal. Chim. Acta* **466** 69

[3] Horrillo M C, Gutiérrez J, Arés L, Robla J I, Sayago I and Getino J 1995 *Sens. Actuators B* **25** 507

[4] Sberveglieri G 1995 *Sens. Actuators B* **23** 103

[5] Kohl D 1989 *Sens. Actuators* **18** 71

[6] Schmidt-Mende L and MacManus-Driscoll J L 2007 *Mater. Today* **10** 40

[7] Jones A, Jones T A, Mann B and Firth J G 1984 *Sens. Actuators* **5** 75

[8] Basu S and Dutta A 1994 *Sens. Actuators B* **22** 83

[9] Sberveglieri G, Nelli P, Groppelli S, Quaranta F, Valentini A and Vasanelli L 1990 *Mater. Sci. Eng. B* **7** 63

[10] Lampe U 1989 *Sens. Actuators* **18** 269

[11] Traversa E and Bearzotti A 1995 *Sens. Actuators B* **23** 181

[12] Hjiri M, El Mir L, Leonardi S G, Donato N and Neri G J 2013 *Nanomaterials* **3** 357

[13] Baratto C, Sberveglieri G, Onischuk A, Caruso B and di Stasio A 2004 *Sens. Actuators B* **100** 261

[14] Prajapati C S, Kushwaha A and Sahay P P 2013 *Mater. Chem. Phys.* **142** 276

[15] Korotcenkov G 2005 *Sens. Actuators B* **107** 209

[16] Han N, Wu X F, Zhang D W, Shen G L, Liu H D and Chen Y F 2011 *Sens. Actuators B* **152** 324

[17] Ozgur U, Alivov Y I, Liu C, Teke A, Reshchikov M A, Doğan S *et al* 2004 *J. Appl. Phys.* **98** 041301

[18] Paraguay F, Miki-Yoshida M, Morales J, Solis J and Estrada W 2000 *Thin Solid Films* **373** 137

[19] Salam S, Mohammad I and Aftab A 2013 *Thin Solid Films* **529** 242

[20] Sun J B, Xu J, Yu Y S, Sun P, Liu F M and Lu G Y 2012 *Sens. Actuators B* **169** 291

[21] Cheng X L, Zhao H, Huo L H, Gao S and Zhao J G 2004 *Sens. Actuators B* **102** 248

[22] Arshak K and Gaidan I 2005 *Mater. Sci. Eng. B* **118** 44

[23] Neri G, Bonavita A, Rizzo G, Galvagno S, Capone S and Siciliano P 2006 *Sens. Actuators B* **114** 687

[24] Sushil Kumar Pandey, Saurabh Kumar Pandey, Vishnu Awasthi, Ashish Kumar, Uday P Deshpande, Mukul Gupta *et al* 2014 *Bull. Mater. Sci.* **37** 983

[25] Vanmathi M, Mohamed I, Marikkannan S K and Venkateswarlu M 2017 *J. Ovonic Res.* **13** 345

[26] Joseph B, Gopichandran K G, Thomas P V, Koshy P and Vaidyan V K 1999 *Mater. Chem. Phys.* **58** 71

[27] Park J H, Jang S J, Kim S S and Lee B T 2006 *Appl. Phys. Lett.* **89** 121108

[28] Chen J J, Yu M H, Zhou W L, Sun K and Wang L M 2005 *Appl. Phys. Lett.* **87** 173119

[29] Yu Z G, Wu P and Gong H 2006 *Appl. Phys. Lett.* **88** 132114

[30] Kamble V B and Umarji A M 2013 *J. Mater. Chem. C* **1** 8167

[31] Peace G S 1993 *Taguchi methods: a hands-on approach* (Massachusetts: Addison-Wesley Reading)

[32] Chen C C, Tsao C C, Lin Y C and Hsu C Y 2010 *Ceram. Int.* **36** 979

[33] Fernández S, Martínez-Steele A and Naranjo F B 2009 *Thin Solid Films* **517** 3152

[34] Tseng C H, Huang C H, Chang H C, Chen D Y, Chou C P and Hsu C Y 2011 *Thin Solid Films* **519** 7959

[35] Hu C C, Lu T W, Chou C Y, Wand J T, Huang H H and Hsu C Y 2014 *Bull. Mater. Sci.* **37** 1275

[36] Kao J Y, Tsao C C, Wang S S and Hsu C Y 2010 *Int. J. Adv. Manuf. Technol.* **47** 395

[37] Noorul Haq A, Marimuthu P and Jeyapaul R 2008 *Int. J. Adv. Manuf. Technol.* **37** 250

[38] Nihat T and Hasim P 2010 *Int. J. Adv. Manuf. Technol.* **46** 509

[39] Patel S R and Murthy Z V P 2010 *Cryst. Res. Technol.* **45** 747

[40] Lee J, Jung H, Lee J, Lim D, Yang K, Yi J *et al* 2008 *Thin Solid Films* **516** 1634

[41] Wu G M, Chen Y F and Lu H C 2011 *Acta Phys. Pol. A* **120** 1

[42] Pignatiello J J J 1988 *IIE Trans.* **20** 247

[43] Chen Y I and Duh J G 1991 *Mater. Chem. Phys.* **27** 427

[44] Jeong S H and Boo J H 2004 *Thin Solid Films* **105** 447

[45] Windischmann H and Mark P 1979 *J. Electrochem. Soc.* **126** 627

[46] Chang J F, Kuo H H, Leu I C and Hon M H 2002 *Sens. Actuators B* **84** 258

[47] Buono-Core G E, Klahn A H, Cabello G and Lillo L 2013 *Polyhedron* **62** 1

[48] Ohyama M, Kozuka H and Yoko T 1988 *J. Am. Ceram. Soc.* **81** 1622.

[49] Pearton S J, Norton D P, Ip K, Heo Y W and Steiner T 2005 *Prog. Mater. Sci.* **50** 293

[50] Zhi Z Z, Liu Y C, Li B S, Zhang X T, Lu Y M, Shen D Z *et al* 2003 *J. Phys. D: Appl. Phys.* **36** 719

[51] Lee J-H and Park B-O 2003 *Thin Solid Films* **426** 94

[52] Shahid M U, Deen K M, Ahmad A, Akram M A, Aslam M and Akhtar W 2016 *Appl. Nanosci.* **6** 235

[53] Pimentel A, Fortunato E, Goncalves T A, Marques A, Aguas H, Pereira L *et al* 2005 *Thin Solid Films* **487** 212

[54] Lin S S, Huang J L and Sajgalik P 2005 *Surf. Coat. Technol.* **191** 286

[55] Yakuphanoglu F, Caglar Y, Ilican S and Cagla M 2007 *Physica B* **394** 86

[56] Lv M, Xiu X, Pang Z, Dai Y and Han S 2006 *Appl. Surf. Sci.* **252** 5687

[57] Lv M, Xiu X, Pang Z, Dai Y and Han S 2005 *Appl. Surf. Sci.* **252** 2006